Theorization and Modeling Ⅲ
(Review)

Crystal Nucleation in Supercooled Liquid Metals

Kenneth F. Kelton

Abstract

It is becoming increasingly clear that nucleation processes in liquids and glasses are more complicated than previously thought, often coupling to other phase transitions and ordering processes. Experimental and theoretical studies show the development of icosahedral short-range order in many supercooled transition metal and alloy liquids, which in some cases extends beyond nearest neighbor distances. This atomic and chemical ordering couples to the nucleation barrier, and may play a role in glass formation in some cases. Select experimental results are presented to demonstrate these points. These are discussed in light of nucleation theories, including the commonly used Classical Theory of Nucleation, diffuse interface theories, and coupled-flux theory, which takes account of the interaction between interfacial processes at the surface of the crystal nuclei and long-range diffusion fluxes.

Keyword(s): nucleation, supercooling, liquid structure, glass formation

1. Introduction

Phase transitions are ubiquitous, ranging from the solidification of liquids, to solid-state transformations, to the precipitation of kidney stones, and even to changes in the early universe. Most of these phase transitions are initiated by a *nucleation* step. In this step large changes in some order parameter, which characterizes the difference between the initial and transformed phases, occurs within spatially small regions. Liquid solidification is often used for the investigation of nucleation processes because strain effects, which complicate nucleation studies in solids, are effectively absent. Under the right conditions liquids can be maintained for long periods of time at temperatures below their equilibrium melting (or liquidus) temperatures, i.e. in a *supercooled* state. That this is possible indicates the existence of a barrier to the formation of the stable crystal phases, generally called the *nucleation barrier*.

As will be shown in this article, even in metallic liquids nucleation is complicated, challenging current understanding. The thermodynamic model that underlies the most commonly used model for nucleation, the Classical Theory of Nucleation, is questionable when applied to the small clusters involved in the nucleation step. Inherent chemical and topological ordering in the volume of the liquid, and ordering near the interface with the growing crystal and near surfaces, are not fully included in nucleation theories, although some progress been has made using density functional approaches. The nucleating phase often has a chemical composition that is different from that of the parent phase, making long-range diffusion effects potentially important. To treat this problem correctly, the stochastic interfacial processes described by most nucleation theories must be coupled with the stochastic diffusion field, which is only rarely done. Finally, there is a great deal of interest in metallic

glass formation, which requires that crystallization be effectively bypassed. An understanding of the kinetics of crystal nucleation during rapid cooling and how nucleation depends on the structural evolution of the liquid is needed to treat this problem. These points are briefly surveyed in this article.

2. Nucleation Theory

Before looking at experimental data, it is useful to discuss briefly the current state of nucleation theory.

2.1 Classical Theory of Nucleation

In *homogenous nucleation*, small regions of crystalline order arise spontaneously by spatially and temporally independent fluctuations within the supercool liquid. In *heterogeneous nucleation* these fluctuations are catalyzed at specific sites. Both types of nucleation are most often analyzed within the Classical Theory of Nucleation (CNT).[1] In homogeneous CNT, small regions of the crystal phase (clusters) develop randomly in space and time by a series of kinetic reactions in which single atoms or molecules (monomers) attach and detach from the cluster interface. Assuming spherical clusters, negligible strain, and a sharp interface between the crystal and amorphous phase, the reversible work of formation of a cluster of n monomers is:

$$W_n = n\Delta\mu + (36\pi)^{1/3}\,\overline{v}^{2/3}\,n^{2/3}\,\sigma \qquad (1)$$

Here $\Delta\mu$ is the Gibbs free energy of the crystal phase less than that of the glass phase per monomer, $\overline{v}$ is the monomer volume, and σ is the liquid-crystal interfacial free energy per unit surface area. The competition between the volume free energy favoring cluster formation and the surface free energy opposing it leads to a maximum in the work of formation, W_{n*}, for a critical cluster size, $n*$. Clusters are assumed to evolve slowly by a series of bimolecular reactions, where the rate of change of the

Department of Physics, Campus Box 1105, Washington University, One Brookings Drive, St. Louis, Missouri 63130 USA
(E-mail: kfk@wustl.edu)

time-dependent population density as a function of the cluster size, n, and time, t, is

$$\frac{dN_{n,t}}{dt} = N_{n-1,t}\,k_{n-1}^+ - N_{n,t}\left[k_n^+ + k_n^-\right] + N_{n+1,t}\,k_{n+1}^- \quad , \qquad (2)$$

where k_n^+ is the rate of monomer addition to a cluster of size n and k_n^- is the rate of monomer loss. Assuming interface-limited kinetics (strictly valid only for nucleation processes where the initial and final phases have the same chemical composition) $k_n^\pm = 4n^{2/3}\gamma_n^\pm$. For spherical clusters, the first term ($4n^{2/3}$) is the number of attachment sites on the surface of the cluster, and, $\gamma_n^\pm = \frac{6D}{\lambda^2}\exp\left(\mp\frac{\delta W_n}{2k_B T}\right)$ where D is the diffusion coefficient in the liquid, λ is the jump distance, k_B is Boltzmann's constant, T is the temperature and $\delta W_n = W_{n+1} - W_n$. The nucleation frequency, $I_{n,t}$, is the time- and size-dependent flux from clusters of size n to ones of size $n+1$ ($I_{n,t} = k_n^+ N_{n,t} - k_{n+1}^- N_{n+1,t}$). Except for extremely rapid cooling rates (see Section 3.3), time-dependent effects are generally not important for crystallization from the liquid, although they can play a very prominent role in glass crystallization[2),3)].

To a lowest approximation, the nucleation rate is the forward flux of clusters past the critical size. To obtain a more quantitative expression, assuming a time-invariant (steady-state) cluster distribution ($N_{n,t} \rightarrow N_n^{st}$), the steady-state nucleation rate is

$$I^{st} = \frac{24D\,(n^*)^{2/3}\,N_A}{\lambda^2}\left(\frac{|\Delta\mu|}{6\pi k_B T n^*}\right)^{1/2}\exp\left(-\frac{W_{n^*}}{k_B T}\right), \qquad (3)$$

where the critical size, n^*, is $32\pi\sigma^3/3\,\bar{v}\,|\Delta g|^3$, the critical work of formation, W_{n^*} (called the *nucleation barrier*) is $16\pi\sigma^3/3\,\bar{v}\,|\Delta g|^2$ (where $\Delta g = \Delta\mu/\bar{v}$), and N_A is the total number of monomers in the system, typically taken to be Avogadro's number per mole (see Ref. 1 for more details). Frequently, solid impurity sites, such as a container wall, lower the value of W_{n^*}, which from Eq. (3) will increase the nucleation rate. Within CNT, this is taken into account by multiplying W_{n^*} by a factor $f(\theta)$ that varies between 0 and 1 depending on the contact angle, θ, between the crystal phase and the solid (see Ref. 1 for a detailed discussion of heterogeneous nucleation).

Equation (3) predicts a sharp increase in the nucleation rate with decreasing temperature due to the increasing driving free energy, followed by a decrease at lower temperatures due to the slowing atomic dynamics. This predicted behavior is in good agreement with experimental data[1),4)]. A fundamental problem with CNT is that the magnitude of the nucleation rate is extremely sensitive to the value of the interfacial energy, which is generally only known from fits to nucleation data.

2.2 Diffuse Interface Theories

The CNT assumes that the interface between the volume and surface contributions to the work of cluster formation can be cleanly divided (Eq. (1)), requiring a sharp interface between the nucleating cluster and the parent liquid phase. However, this interface is actually diffuse [5)-7)], with a width that is of the order of the radius of the nucleation clusters when the driving free energy is large. The regions of the liquid near the cluster are, therefore, more ordered than expected within CNT.

A phenomenological model to account for the ordering was proposed independently by Gránásy[8)-10)] and Spaepen[11)]. Ordering in the liquid ahead of the advancing cluster interface implies that the Gibbs free energy $g(r)$ will change continuously on crossing the cluster boundary. To lowest order, this can be described by the step-function shown in **Fig. 1**, allowing the work of cluster formation to be readily obtained,

$$W_{n^*} = \frac{4\pi}{3}\Delta g_{il}\,\delta^3\,\frac{b^2}{(1-b)^2} \qquad (4)$$

where δ is the interfacial width, $b^2 = 1 - (\Delta g_{sl}/\Delta g_{il})$, Δg_{sl} is the free energy difference of the liquid and solid phases ($g_s - g_l$), and Δg_{il} is the free energy difference between the liquid and interface ($g_i - g_l$). By Equating this value for W_{n^*} with that obtained from the CNT, an expression for the interfacial free energy is obtained, $\sigma_{ls} \approx \delta(\Delta g_{il} - \Delta g_{sl}/2)$. A key result from this model is that σ_{ls} is predicted to have a positive temperature dependence in agreement with experiment [12)]. Here, a simplistic profile was considered. The precise profile of $g(r)$ can be obtained from a density-functional theory (DFT) approach in terms of one or more order parameters that characterize the initial and transformed phases.

In principle a DFT formalism can also be used to account for coupling of nucleation processes to other phase transitions in the parent phase (such as chemical or magnetic ordering transitions). For illustration, consider the semi-empirical density functional
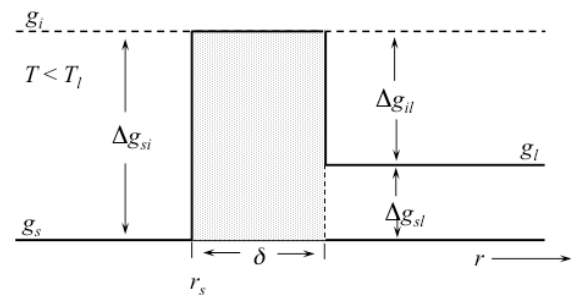
Fig. 1 Step-function change of the free-energy density through the interfacial region between the liquid and solid (from r_s to $r_s + \delta$. (Adapted from Ref. 11, copyright (1994), with permission from Elsevier.)

approximation (SDFA), where a single order parameter, M, is assumed. In the liquid far from the cluster, $M(r,t)$ is zero; it is equal to one for an infinitely large solid cluster. The free energy can be written as a functional of M, $G[M(r,t)]$, and the work of cluster formation can be computed in a similar way as from the CNT, $W[M] = \int_V \left(g(M(r,t)) - \mu(M(r,t))\right) dr$ (see Refs. 1 and 13) for a detailed treatment). **Figure 2** shows the computed order parameter, M, as a function of distance from the center of the cluster for three different values of $\tilde{\Delta}$, which is a scaled parameter that corresponds to the driving free energy. The values for $\tilde{r}_s^*$, the corresponding scaled critical radii, are listed in the figure. Like the CNT, increased magnitudes of the driving free energy give smaller values for the critical size. However, for all values of $\tilde{\Delta}$ the interface is diffuse. As shown in the inset, only when $\tilde{\Delta}$ becomes very small (= -0.05, corresponding to $\tilde{r}_s^* = 20$) does the interface approach the sharp boundary assumed in CNT. Further, although M should be unity in the solid phase, it does not reach that value even in the center of the cluster, except when the driving free energy is very small. Calculations also show that the CNT overestimates the work of cluster formation for larger driving free energies. Taken together, these results indicate that the CNT is only quantitatively correct when the departure from equilibrium is small, i.e. near the melting (or liquidus) temperature. Although not discussed here, studies show that the DIT and SDFA models fit nucleation rate data in liquids and glasses better than the CNT, demonstrating the importance of the ordering in the liquid near the cluster interface[1), 14].
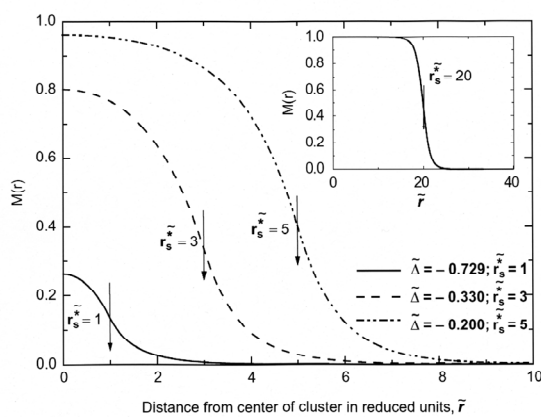
2.3 Coupled Flux Theory - Incorporation of Long-Range Diffusion

The nucleation theories previously discussed are interface-limited theories, appropriate if the chemical composition of the nucleating phase is the same as that of the liquid (polymorphic crystallization), or if the diffusion rates in the liquid are much faster than the interfacial attachment kinetics. The latter can make CNT particularly inappropriate for solid-state precipitation [15),16)], but it is generally not an important issue for nucleation from the liquid if the temperature is constant or slowly varying. When the interfacial attachment rates to the cluster do become competitive with the diffusive transport rates in the liquid, these two stochastic fluxes become coupled.

Following an approach first suggested by Russell [18)], this may be treated to lowest order by focusing attention on three regions **(Fig. 3)**: the cluster, the immediate neighborhood around the cluster (the shell region), and the parent phase [17),19)]. In this *Coupled*-Flux Model (CFM), the flux between the shell and the parent phase is coupled with that between the shell and the cluster. The cluster evolution underlying time-dependent nucleation is determined by solving numerically a system of coupled differential rate equations that incorporate the interfacial and shell/parent phase fluxes. Numerical solutions show that the coupled-fluxes can significantly lower the nucleation rate and increase the induction time for nucleation beyond the predictions from the CNT. Surprisingly, a key prediction of CFM is that for sub-critical clusters, the liquid composition is closer to that of the precipitating cluster, in contradiction with expectations based on the growth of large clusters. These predictions have been confirmed in Kinetic Monte Carlo simulations that probe the growth and shrinkage of clusters in a simple lattice gas model, augmented with adjustable diffusion kinetics [20)].

While coupling of the interfacial and diffusive fluxes typically has little influence on nucleation from supercooled
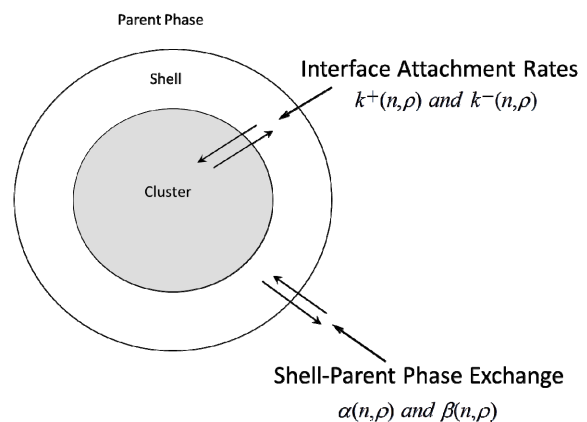

Fig. 2 Order parameter M as a function of the scaled distance from the center of the critical cluster. Profiles are shown for three different values of the scaled driving free energy, $\left|\tilde{\Delta}\right|$. (Reprinted from Ref. 13, copyright (1994), American Institute of Physics.)


Fig. 3 A schematic illustration of the fluxes in the Coupled-Flux Model. (Reprinted from Ref. 17, copyright (2000) with permission from Elsevier.)

liquids, it can have a significant effect for nucleation during a rapid quench (see Section 3.3) and in glass devitrification [21]. Coupled-flux effects may also be important for nucleation under quiescent micro-gravity conditions, where stirring (which is always present in a terrestrial environment) is suppressed.

3. Nucleation Studies in Metallic Liquids

3.1 Experimental Techniques

Heterogeneous nucleation, on impurities in the liquid or on the container walls, generally dominates the solidification of liquid metals. Since the number of heterogeneous sites and their catalytic efficiencies are generally unknown, a quantitative analysis of such nucleation data is difficult or impossible. For this reason, techniques have been developed to minimize the impact of heterogeneous nucleation, so that homogeneous nucleation may be studied (see Refs. 1 and 4 for a more extended discussion than provided here). These include (i) *isolation*, where impurities are compartmentalized into a small volume fraction of the liquid[12),22),23)], (ii) *fluxing*, where the liquid is coated with a material that dissolves or renders ineffective impurities and protects it from the container walls and (iii) *containerless processing*, where liquids are held without containers in vacuum or a high-purity non-oxidizing atmosphere. The most common containerless techniques are based on aerodynamic levitation, electromagnetic levitation (EML) and electrostatic levitation (ESL) [1),24)]. Aerodynamic levitation is achieved by a controlled gas flow through nozzles of optimal design for the size and density of the samples of interest. However, the flowing gas makes temperature and positioning control difficult, may lead to heterogeneous nucleation on gas impurities, and cannot be used for quantitative measurements of thermophysical properties. EML uses a high frequency EM field to induce eddy currents in metallic samples, providing levitation from Lenz's law. However, since both heating and levitation are coupled in EML[24], it is not always possible to supercool the liquid while maintaining sample levitation under terrestrial conditions. Further, only metallic materials, or semiconducting materials that become metallic in the liquid phase (e.g. Si), can be studied. Electrostatic levitation (ESL) is the most versatile, offering several key advantages over aerodynamic and electromagnetic levitation: (1) non-metallic as well as metallic systems can be studied; (2) the heating and positioning power are decoupled, allowing measurements in more deeply supercooled liquids; and (3) the rf coils required for electromagnetic levitation limits the view of the sample while ESL provides a wide range of access to the sample. In ESL charged samples with a 2.0 – 3.0 mm diameter (approximately 30-70 mg mass) are levitated by Coulomb forces in an electrostatic field (0 to 2 MV/m) under high vacuum (typically $10^{-7} – 10^{-8}$ torr) [25), 26)]. The samples are initially
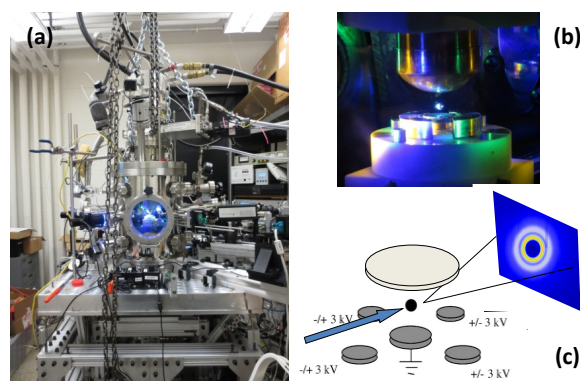
Fig. 4 (a) Photograph of the ESL at Washington University, optimized for X-ray scattering studies. (b) A levitated sphere; the different colors of light are from the high-intensity LEDs used in the sample positioning feedback algorithm. (c) Schematic diagram showing the incoming and scattered X-rays in a transmission geometry from a levitated liquid sample; the diffraction pattern is recorded on an area detector. The vertical and two sets of side electrodes used for levitation and positioning are also shown (*c* is courtesy of N. A. Mauro).

charged by induction. During processing the charge is maintained with an external UV source at low temperatures and by thermionic emission at high temperatures. Three pairs of orthogonal electrodes and a robust control algorithm[27),28)] maintain the sample position during processing to within 50-100 μm, based on error signals from two orthogonal position-sensitive detectors, which are provided as input to the DC amplifiers connected to the electrodes. The sample can then be heated to any temperature up to ≥ 3000 K using one or more lasers. Our liquid diffraction data, some discussed in this review, were obtained using an ESL facility (WU-Beamline ESL, or WU-BESL) (**Fig. 4**) that has been constructed at Washington University and optimized for X-ray diffraction studies of the levitated supercooled liquids [29]. A schematic of the transmission X-ray diffraction geometry is shown in **Fig. 4.c**. Complementary physical property data, such as maximum supercooling, density, surface tension and viscosity, can be obtained in ESL, allowing the liquid structure to be linked with the crystal nucleation barrier (Section 4) and with thermophysical properties.

3.2 Maximum Undercooling Results for Elemental Liquids

Since, as demonstrated in studies of nucleation in silicate glasses, the steady-state nucleation rate rises rapidly with supercooling [4], and the growth velocities in the supercooled liquid are large, the time scale for crystallization is dominated by the time required to form a nuclei. Experimental studies show that the *reduced undercooling* ($\Delta T_r = (T_m − T_u)/T_m$, where T_m is the melting temperature and T_u is the minimum